International Journal of Mechanical, Industrial and Aerospace Sciences
ISSN: 2517-9950
Vol:8, No:9, 2014

Design and Evaluation of a Pneumatic Muscle Actuated Gripper

Tudor Deaconescu, Andrea Deaconescu

***Abstract*—**Deployment of pneumatic muscles in various industrial applications is still in its early days, considering the relative newness of these components. The field of robotics holds particular future potential for pneumatic muscles, especially in view of their specific behaviour known as compliance. The paper presents and discusses an innovative constructive solution for a gripper system mountable on an industrial robot, based on actuation by a linear pneumatic muscle and transmission of motion by gear and rack mechanism. The structural, operational and constructive models of the new gripper are presented, along with some of the experimental results obtained subsequently to the testing of a prototype. Further presented are two control variants of the gripper system, one by means of a 3/2-way fast-switching solenoid valve, the other by means of a proportional pressure regulator. Advantages and disadvantages are discussed for both variants.

***Keywords*—**Gripper system, pneumatic muscle, structural modeling.

I. Introduction

PREHENSION, as a general action, includes grabbing and seizing with fingers, claws or tweezers of objects, in view of repositioning. While, as suggested by this assertion, this action is characteristic primarily to living natural systems, biomimetics helped conceive artificial gripper systems, also known as “mechanical hands”.

Mechanical hands are meant to replace human ones, their required abilities being dictated by the large variety of applications. Thus, studies have revealed that related to the 100% gripping ability of a five-finger mechanical hand, this decreases to 99% in a four-finger one, to about 90% in a three-finger and to mere 40% in a two-finger hand [1].

Gripper systems represent the final elements in robotic structures and are often not included by their “anatomy”. Their role is to facilitate temporary contact with the manipulated object, ensuring its position and orientation during transport and specific activities [2], [3]. The characteristic motions of prehension are generated by means of motors that have to fulfil the mean tasks of such a system, like ensuring a sufficient clamping force, precision, reliability, flexibility, compliance etc. By the type of energy used by the motors, these can be electrical, hydraulic, pneumatic or non-conventional [4].

Pneumatic actuation is the one most frequently encountered in the construction of gripper systems, due to certain advantages like using a non-polluting working environment, the possibility of overloading the system, easy adjusting of forces, torques, speeds, compliant behaviour etc. [5]. Linear or rotating pneumatic motors combined with mechanical systems for the transmission of motion ensure the mobility of the fingers by straight or curved trajectories, as demanded by any concrete application.

Over the last years membrane type pneumatic motors (pneumatic muscles) have benefitted from continued development for the generation of both linear and circular motion. Pneumatic muscles stand out by valuable properties like their shock-absorbing capacity, low weight, small size, reduced mass-to-power unity ratio and elasticity (springlike behaviour) due to air compressibility on one hand, and variation of force with displacement on the other. Such characteristics render pneumatic muscles optimum constructive elements for the construction of gripper systems.

Linear pneumatic muscles have been commercialised by the Bridgestone Rubber Company of Japan starting 1980 and more recently, by the American Shadow Robot Company and the Festo Corporation of Germany [6]-[8]. A rotating chamber type pneumatic muscle has been developed at Bremen University in Germany in order to generate rotation by a circular arc of limited angle. Its construction is based on series-connecting several chambers made from welded plastic foils communicating via a channel through that compressed air is fed to the system. A higher compressed air pressure will generate a greater rotation angle of the system [9], [10].

At present construction of gripper systems driven by pneumatic muscles is limited, because of insufficient knowledge of these actuators. One of the gripper systems whose actuation deploys a linear pneumatic muscle is called Power Gripper and is manufactured by Festo. Its working principle mimics the seizing of objects by birds using their beaks, and its construction is based on Watt linkages. Fig. 1 shows a view of such a gripper system [11].

Fig. 1 Power Gripper

Prof. Dr. Eng. Tudor Deaconescu and Prof. Dr. Eng. Andrea Deaconescu are with the Transilvania University of Brasov, Faculty of Technological Engineering and Industrial Management, Department of Industrial Engineering and Management, Bd. Eroilor 29, Romania, RO-500036 (phone: 0040-268-477113; fax: 0040-268-477113; e-mail: tdeacon@ unitbv.ro, deacon@ unitbv.ro).

Fig. 2 Parallel gripper system

The Power Gripper has an excellent developed force-to-eigenweight ratio, due to the light materials of its structure (aluminium) and to the reduced weight of the pneumatic muscle.

Another construction developed also by Festo is a parallel gripper of DMSP-...-HGP-SA type actuated by two pneumatic muscles. It was designed for pick-and-place operations to be conducted in environments with high dust content (Fig. 2) [12].

Other several parallel and radial pneumatic muscle actuated gripper system variants are those developed at Transilvania University of Braşov in Romania [13]. Their construction includes in the same casing the mechanical actuation system as well as the pneumatic proportional control apparatus.

Further on an innovative constructive variant of a gripper system will be presented and discussed, based on actuation by a linear pneumatic muscle. Following the introduction of Section I, the paper addresses the structural, kinematic and static models of the gripper system in section II, discusses the constructive model in Section III, and the functional characteristics of the analysed system in Section IV. Section V deals with certain experimental results obtained for the gripper system prototype, followed by conclusions in Section VI.

II. Structural, Kinematic and Static Modelling of the Gripper System

The construction of gripper systems tends to become more and more complex, what entails increasing costs, difficult to accept in the context of a competitive industrial scenario [14].Starting from this consideration, the paper presents and discusses a gripper system actuated by a linear pneumatic muscle, a light and compliant bio-inspired element. The power transmission mechanism is asymmetrical, consisting of a gear and rack mechanism, which transmits and distributes the input motion from the pneumatic muscle to the two jaw-supports.

The proposed gripper system has two fingers (jaws) with one degree of mobility each, suitable for industrial applications of manipulating fragile objects or for certain medical applications (Fig. 3). Power is transmitted to the two jaw-supports by gears and racks; the entire assembly was sized based on the following input data: mass of the gripped object: m = 0.7 kg; acceleration of the gripper + object system's motion: a = 5 m/s^2; gravitational acceleration: g = 9.81 m/s^2; emergency stopping deceleration: a_S = 10 m/s^2; friction coefficient: μ = 0.2; safety coefficient: S = 2.5.

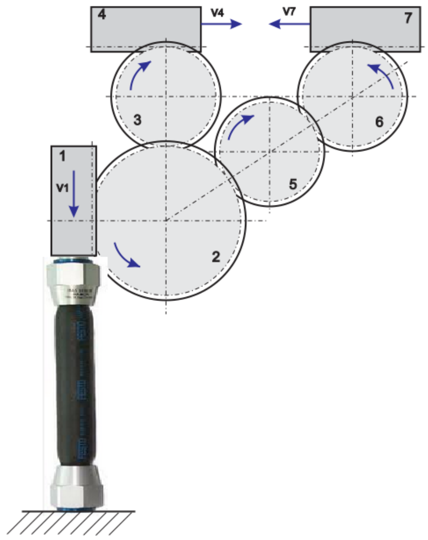

Fig. 3 Parallel asymmetric gripper system with two mobile jaws

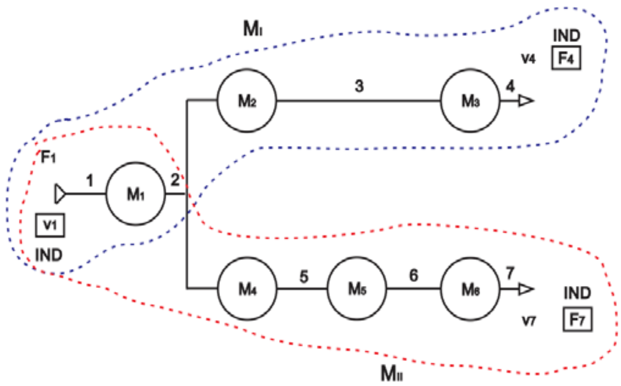

Fig. 4 Block diagram of the gripper system

Fig. 4 shows the block diagrams of the above gripper system. The analysed gripper system includes two parallel-connected linkages (M_I and M_{II}) that branch out at gear 2. The number of exterior links of the studied mechanical system is L = 3, meaning that three inputs and outputs of the system are available. Input to the system is the exterior link of the mechanism to the motor (pneumatic muscle) and is characterised by a speed (v_1) and a force (F_1) that have the same direction. The two outputs of the system represent its exterior links to the jaw-supports of the gripper; they are characterised each by a speed (v_4 and v_7, respectively) and a force (F_4 and F_7, respectively), of opposite directions.

The two linkages are coupled at gear 2 (L_C = one coupling), what entails elimination of an independent motion. In this case the degree of mobility of the entire assembly is:

$$M = \sum M_k - L_c = M_I + M_{II} - L_C = 1 + 1 - 1 = 1 \qquad (1)$$

The conceived gripper system uses the following gears and racks: gear module = 1 mm; z_2 = 30 teeth (cogs); $z_3 = z_5 = z_6$ = 20 teeth (cogs).

A. Determination of the Transmission Functions of Speeds

Further on the transmission ratios of all gears of the gripper system are presented and deduced, respectively:

$$i_{12} = \frac{v_1}{\omega_2} = \frac{\omega_2 \cdot R_2}{\omega_2} = R_2 = \frac{m \cdot z_2}{2} = \frac{1 \cdot 30}{2} = 15 \quad (2)$$

where m is the module of the gear, ω_i – the angular velocity of gear i, and R_i – the radius of the pitch circle of gear i.

Transmission ratios i_{23}, i_{25} and i_{56} are computed by (3) to (5):

$$i_{23} = \frac{\omega_2}{\omega_3} = -\frac{z_3}{z_2} = -\frac{20}{30} = -\frac{2}{3} \quad (3)$$

$$i_{25} = \frac{\omega_2}{\omega_5} = -\frac{z_5}{z_2} = -\frac{20}{30} = -\frac{2}{3} \quad (4)$$

$$i_{56} = \frac{\omega_5}{\omega_6} = -\frac{z_6}{z_5} = -\frac{20}{20} = -1 \quad (5)$$

and transmission ratios i_{34} and i_{67} are computed by (6) and (7):

$$i_{34} = \frac{\omega_3}{v_4} = \frac{\omega_3}{\omega_3 \cdot R_3} = \frac{1}{R_3} = \frac{2}{m \cdot z_3} = \frac{2}{1 \cdot 20} = \frac{1}{10} \quad (6)$$

$$i_{67} = \frac{\omega_6}{v_7} = \frac{\omega_6}{\omega_6 \cdot R_6} = \frac{1}{R_6} = \frac{2}{m \cdot z_6} = \frac{2}{1 \cdot 20} = \frac{1}{10} \quad (7)$$

Starting from the above computed results, the global transmission ratios of the two linkages M_I and M_{II} are determined by (8) and (9):

$$\mathrm{i}_{14} = \mathrm{i}_{12} \cdot \mathrm{i}_{23} \cdot \mathrm{i}_{34} = 15 \cdot \left(-\frac{2}{3}\right) \cdot \left(\frac{1}{10}\right) = -1 \quad (8)$$

$$\mathrm{i}_{17} = \mathrm{i}_{12} \cdot \mathrm{i}_{25} \cdot \mathrm{i}_{56} \cdot \mathrm{i}_{67} = 15 \cdot \left(-\frac{2}{3}\right) \cdot (-1) \cdot \left(\frac{1}{10}\right) = +1 \quad (9)$$

from where follow the transmission functions of speeds:

$$\mathrm{v}_4 = \frac{\mathrm{v}_1}{\mathrm{i}_{14}} = -\mathrm{v}_1 \quad (10)$$

$$\mathrm{v}_7 = \frac{\mathrm{v}_1}{\mathrm{i}_{17}} = \mathrm{v}_1 \quad (11)$$

The latter two equations show that output speeds v_4 and v_7 are equal and of opposing directions.

B. Determination of the Transmission Function of Forces

This analysis considers the case where frictions are not neglected; frictions are accounted for by introducing an efficiency coefficient for each gear. Thus the imposed efficiency is of 0.95 for the gears and of 0.97 for the pinion-rack mechanism.

As the number of mechanisms composing the two branches is not equal, the studied aggregate is of *non-homogeneous mixed type*. Fig. 5 shows its diagram.

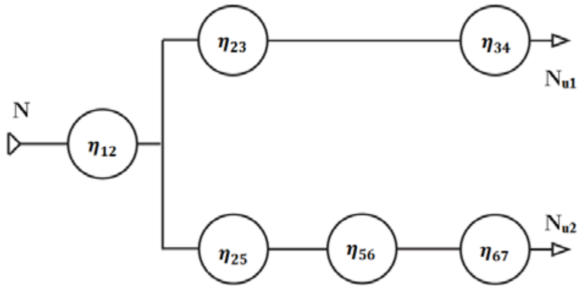

Fig. 5 Non-homogenous diagram of the aggregate with two parallel-connected mechanisms

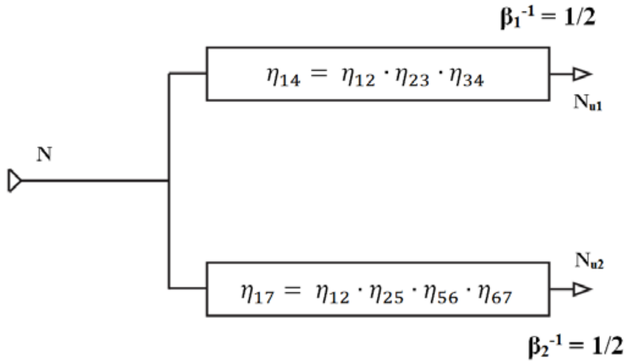

Fig. 6 Associated homogenous diagram

To the non-homogenous diagram can be associated a homogenous one, energetically equivalent, called associated homogenous diagram (Fig. 6).

In Fig. 6 β_i (i = 1,2) denotes the distribution coefficient of the output powers. Equations (12) and (13) are attributed to coefficient β_i [15]:

$$\beta_i = \frac{N}{N_{ui}} \geq 1 \quad (12)$$

$$\sum_{i=1}^{k} \beta_i^{-1} = 1 \quad (13)$$

where N is the input power, N_{ui} are the output powers and k is the total number of the analysed mixed aggregate.

The efficiency of the analysed mixed aggregate is determined by matrix calculus. To the associated homogenous diagram is attached an array containing the distribution coefficients onto branches and the partial efficiencies ordered by the connection of the component linkages. This array is called associated matrix and is presented in (14):

$$[M_\beta] = \begin{bmatrix} \beta_1^{-1} & \eta_{12}^{-1} & \eta_{23}^{-1}\eta_{34}^{-1} & 1 \\ \beta_2^{-1} & \eta_{12}^{-1} & \eta_{25}^{-1}\eta_{56}^{-1} & \eta_{67}^{-1} \end{bmatrix} \quad (14)$$

In this case the efficiency of the aggregate is computed by (15):

$$[\eta^{-1}] = \sum_c \left(\prod_l [M_\beta]\right) \quad (15)$$

where the following two operators have been introduced:

- product by row operator $\prod_l [M_\beta]$:

$$\Pi_l[M_\beta] = \begin{bmatrix} \beta_1^{-1} \cdot \eta_{12}^{-1} \cdot \eta_{23}^{-1} \cdot \eta_{34}^{-1} \cdot 1 \\ \beta_2^{-1} \cdot \eta_{12}^{-1} \cdot \eta_{25}^{-1} \cdot \eta_{56}^{-1} \cdot \eta_{67}^{-1} \end{bmatrix} \quad (16)$$

- sum by column operator Σ_C:

$$\Sigma_C[\beta_1^{-1} \cdot \eta_{12}^{-1} \cdot \eta_{23}^{-1} \cdot \eta_{34}^{-1} \cdot 1 + \beta_2^{-1} \cdot \eta_{12}^{-1} \cdot \eta_{25}^{-1} \cdot \eta_{56}^{-1} \cdot \eta_{67}^{-1}] \quad (17)$$

The efficiency of the analysed gripper system will be:

$$\eta = 1.1481^{-1} = 0.8709$$

Knowing the magnitude of the efficiency, the transmission function of forces is determined starting from the equations below:

$$F_1 \cdot v_1 \cdot \eta + F_4 \cdot v_4 + F_7 \cdot v_7 = 0 \quad (18)$$

and

$$F_1 = \frac{1}{\eta} \cdot \left(-F_4 \cdot \frac{v_4}{v_1} - F_7 \cdot \frac{v_7}{v_1}\right) = \frac{1}{\eta} \cdot \left(-F_4 \cdot \frac{1}{i_{14}} - F_7 \cdot \frac{1}{i_{17}}\right) = \frac{1}{\eta} \cdot (F_4 - F_7) \quad (19)$$

$$F_1 = \frac{F_4 - F_7}{0,8709} \quad (20)$$

III. Constructive Modelling of the Gripper System

Knowing the sequence of motions to be carried out by the gripper system in order to manipulate an object, the least favourable situation is assumed to be sudden braking of the entire assembly, when the gripping force F_G is computed by (21) [3]:

$$F_G = \frac{m \cdot (g + a_S) \cdot S}{\mu \cdot n} = \frac{0,7 \cdot (9,81 + 10) \cdot 2,5}{0,2 \cdot 2} = 86.67\ N \quad (21)$$

Taking into consideration that at the jaw-supports the two forces of opposite directions, F_4 and F_7, have close values ($F_4 = 1.053 \cdot F_7$) and that each is equal to F_G, force F_1 is determined that has to be generated by the pneumatic muscle:

$$\mathrm{F_1} = \frac{\mathrm{F_4} - \mathrm{F_7}}{0.8709} = \frac{173.34}{0.8709} = 199.035\ [N] \quad (22)$$

Conditions imposed on the gripper system are small overall dimensions and minimum weight, what leads to the idea of using a small size pneumatic muscle. A muscle made by Festo AG&Co, Germany (code MAS-10-45N-AA-MC-O-ER-EG) is used, of 10 mm diameter and 45 mm length of the active part. Fig. 7 shows the graph describing the evolution of the force developed by this muscle versus the charging pressure and the stroke.

The maximum allowed contraction such as to ensure the required force can be extracted from the characteristic diagram of the selected pneumatic muscle. In the analysed concrete case, for 0.6 MPa pressure of the compressed air, the contraction of the pneumatic muscle is of 4 mm, what causes the two jaw-supports to drive closer by 8 mm.

The construction of the gripper system is asymmetric, allowing mounting in the same casing of the mechanical assembly and the pneumatic control elements. Fig. 8 shows the location of the components.

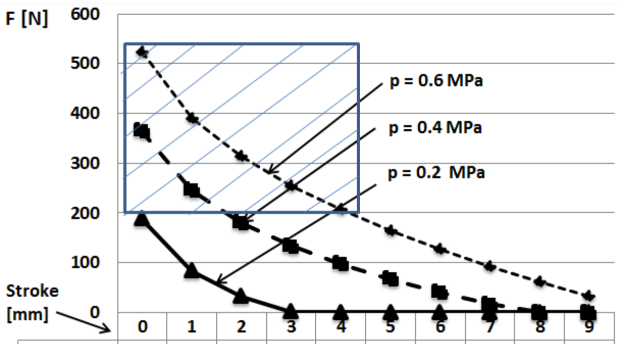

Stroke [mm]	0	1	2	3	4	5	6	7	8	9
p = 0.6 Mpa	522.5	390.8	313.1	255.2	207	164.9	127.2	92.9	61.5	32.4
p = 0.4 Mpa	364.3	245.5	180	134.1	97.8	67.3	40.8	17.3	0	0
p = 0.2 Mpa	187.9	83.2	32.3	1.2	0	0	0	0	0	0

Fig. 7 Variation of the developed force versus charging pressure and stroke

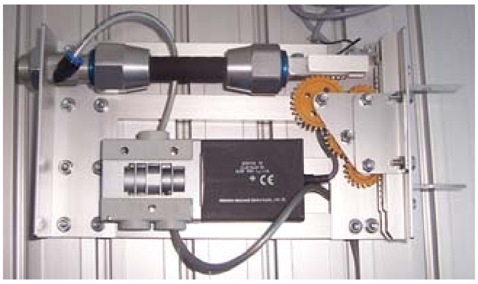

Fig. 8 Construction of the gripper system

IV. Functional Modelling of the Gripper System

The functional model of the gripper system (Fig. 9) was devised in the SimMechanics module of Matlab, and comprises also the kinematic structure of the mechanical assembly, as well as the dimensional parameters of its components.

The seizing motion of the gripper system is generated by a *Sine Wave* type block, which was selected due to the similarity of the pneumatic muscle's motion behaviour to a sine wave. The output quantity of this block is linear and is applied to Rack 1. Its form is given by (23):

$$s(t) = A \cdot \sin(\omega t + \varphi) = 9 \cdot \sin\frac{\pi}{2} t\ [mm] \quad (23)$$

where A is the amplitude of the motion, ω – its pulsation, and φ is the initial phase.

By applying the above described sine signal for 2 seconds, the movement of Rack1 is visualised on a Scope block and described in the graphs of Fig. 10.

The free end of the muscle and thus Rack 1 in the direction of the clamping force takes part in the first part of the imposed working cycle. For this operational sequence an initial sudden leap of the speed can be observed, up to a value of about 14.1 mm/s, after which the motion unfolds smoothly, shock-free, until zero speed is reached, corresponding to the firm gripping of the targeted object. In the second part of the working cycle speed gains again, in the opposite direction, thus allowing release of the gripped object. The maximum acceleration of the free end of the pneumatic muscle records an initial impulse of 353 mm/s^2, corresponding to the speed leap, after which the maximum amplitude of this motion parameter does not exceed 22.1 mm/s^2. These initial leaps are generated by the sudden penetration of the pneumatic muscle by compressed air and can be avoided by rigorous control of the feeding pressure.

For a 9 mm contraction of the pneumatic muscle (the maximum possible stroke), the rotation angles of the gears are of α = 34.37º for gear 2, and of α = 51,56º for gears 3, 5 and 6.

The final elements of the two branches are the jaw-supports 4 and 7. Their displacements [mm], speeds [mm/s] and accelerations [mm/s^2] versus time are plotted in Fig. 11.

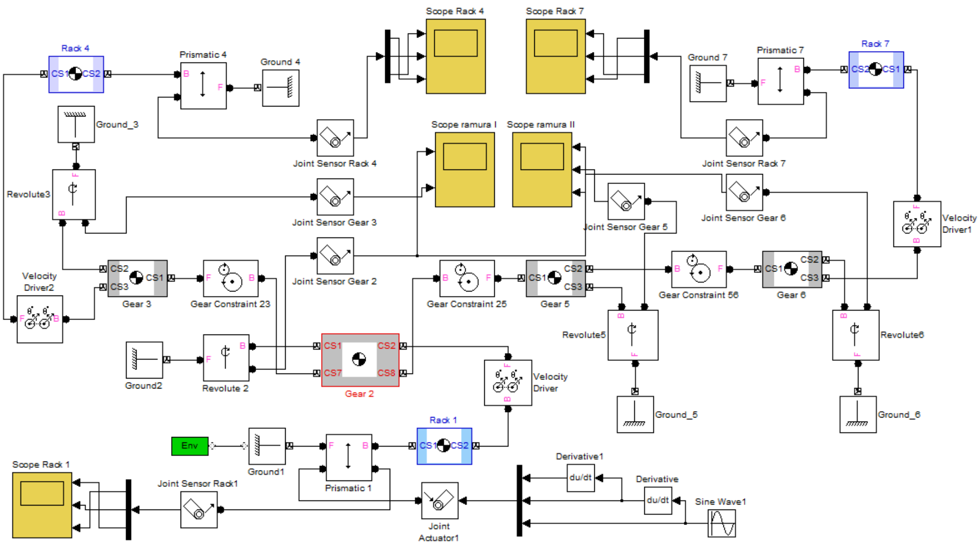

Fig. 9 Functional model of the gripper system

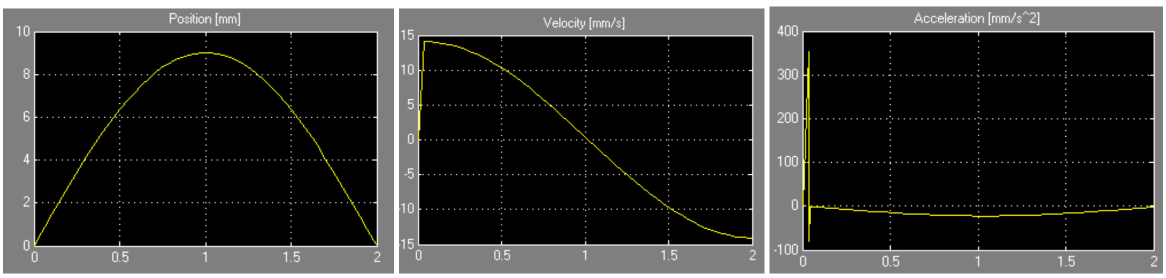

Fig. 10 Position, speed and acceleration of Rack 1

International Journal of Mechanical, Industrial and Aerospace Sciences
ISSN: 2517-9950
Vol:8, No:9, 2014

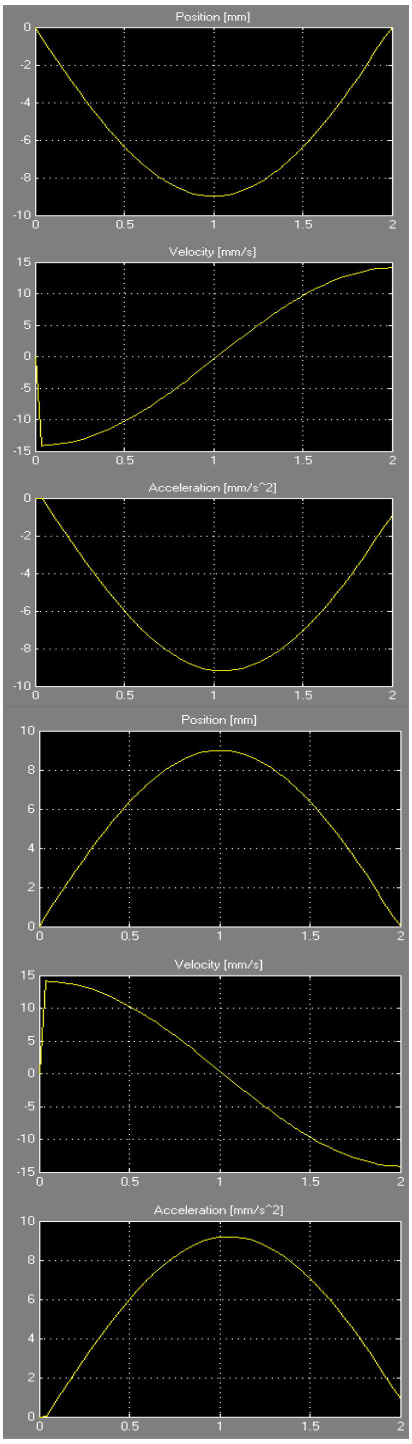

Fig. 11 Evolution of displacements [mm], speeds [mm/s] and accelerations [mm/s^2] of jaw-supports 4 and 7 versus time

In this case too at the beginning of motion for a very short interval of 0.04 s the initial leaps of speeds up to 14.1 mm/s can be observed. The maximum acceleration of the motion is of 9.19 m/s^2.

V. Actuation of the Gripper System

Fig. 12 presents the actuation diagram of the gripper system. The contraction of the pneumatic muscle is controlled by means of a 3/2-way fast-switching normally closed solenoid valve, manufactured by Festo.

The evolution of pressure with the pneumatic muscle versus time was studied for the proposed gripper system for object seizing and realising operations (Fig. 13). Measurements were carried out by means of an analogous pressure gauge connected to the computer via a digital/analogous EasyPort measurement interface. The role of the FluidLab®-P V1.0 programme is to plot the evolution versus time of the analysed parameters.

The motion onset of the pneumatic muscle free end is characterised, as expected also following analysis of the functional model, by the occurrence of a short pressure impulse of 0.086 MPa amplitude and 0.019 s duration. After the imposed pressure has been reached, its value records only small deviations, the maximum amplitude of such fluctuations being 0.0029 MPa, of no relevance to the quality of gripping.

In the case where the 3/2-way fast-switching normally closed solenoid valve is replaced by a proportional pressure regulator of MPPES type also manufactured by Festo, the output pressure will be proportional to a pre-set value of the input quantity, which has the form of a voltage type signal.

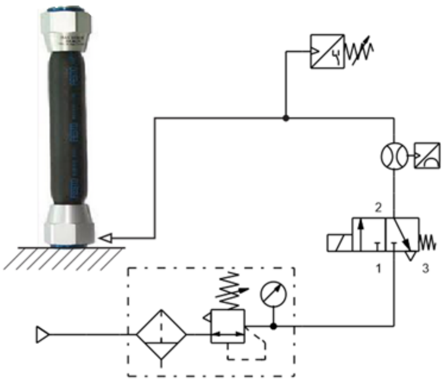

Fig. 12 Actuation diagram of the gripper system

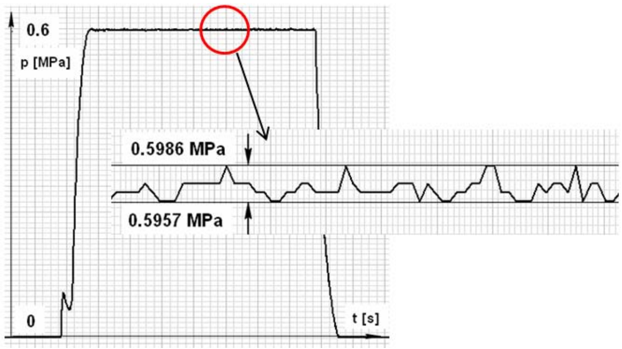

Fig. 13 Evolution of the pneumatic muscle feeding pressure

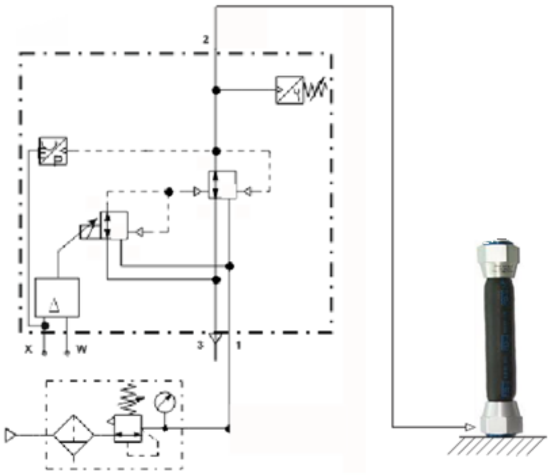

Fig. 14 Actuation diagram of the gripper system including a proportional pressure regulator

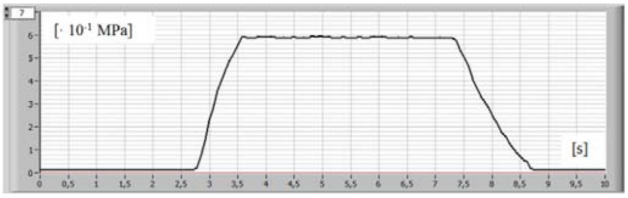

Fig. 15 Evolution versus time of pressure in the pneumatic muscle

The proportional pressure regulator provides a 10 V DC output which can be applied across an external potentiometer to produce a voltage signal setpoint input. By means of this potentiometer the output pressure of the regulator is controlled, and thus the stroke carried out by the pneumatic muscle. Fig. 14 shows the actuation diagram of the gripper system in this case.

For this gripper system too, the evolution versus time of pressure inside the pneumatic muscle for object seizing/releasing operations were studied (Fig. 15).

In this case a positive element should be highlighted, namely the absence of the initial pressure impulse. The downside of this solution is given by the relatively closely occurring pressure pulsations, of even double amplitude, namely 0.0058 MPa. Such values are however not able to compromise the quality of object gripping between the jaws.

VI. Conclusions

The paper presents a new constructive solution of a gripper system, actuated by a pneumatic muscle. The proposed variant is based on the utilisation of a linear pneumatic muscle as motion generating element and on motion transmission towards the jaws by means of gears and racks. The main advantages of the proposed gripper system are small weight and low cost, as well as easy mounting on the various existing robots.

The paper presents structural, constructive and functional models of the gripper, and the simulated motions of its main components. The gripper prototype was tested in two situations, being controlled by a 3/2-way fast-switching solenoid valve, and then by a proportional pressure regulator. For both working variants advantages and disadvantages were identified and discussed. Consequently to the conducted studies it can be asserted that the new gripper system represents an adequate solution in current robotics.

References

[1] C. Stăncescu, *Theoretical and Experimental Study of Gripper Systems with Jaws used in Industrial Robots*, PhD thesis, Transilvania University of Braşov, 2009.

[2] I. Stareţu, *Gripper Systems* (in Romanian). Lux Libris, Braşov, 2010.

[3] G.J. Monkman, S. Hesse, R. Steinmann, H. Schunk, *Robot Grippers*. WILEY-VCH Verlag GmbH & Co. KGaA, Weinheim, 2007.

[4] S. Hesse, *Grippers and their Applications*. Blue Digest on Automation. © 2004 by Festo AG & Co. KG.

[5] H. Murrenhoff, *Fundamentals of Fluid Technology. Part 2: Pneumatics* (in German), Shaker Verlag, Aachen, 2006.

[6] Biorobotics - Build Your Own Robotic Air Muscle Actuator, http://www.imagesco.com/articles/airmuscle/AirMuscleDescription01.html

[7] Shadow Air Muscles, http://www.shadowrobot.com/products/air-muscles/

[8] Festo AG & Co., *Fluidic Muscle MAS, with Screwed Connections*, Catalogue, 2005.

[9] M. Mihajlov, *Modelling and Control Strategies for Inherently Compliant Fluidic Mechatronic Actuators with Rotary Elastic Chambers*, Ph.D. thesis, Institute of Automation, University of Bremen, Germany, 2008.

[10] A. Wilkening, D. Baiden, O. Ivlev, “Assistive Control of Motion Therapy Devices Based on Pneumatic Soft-Actuators with Rotary Elastic Chambers”, *Proceedings of "IEEE International Conference on Rehabilitation Robotics*", ICORR, pp. 1-6, Zürich, 2011.

[11] Festo. PowerGripper – Research project for the development of new gripper systems. http://www.festo.com/cms/en_corp/12728.htm

[12] DMSP-…-HGP-SA Muscle Gripper. Festo. SA 234717 Product Catalogue. https://www.festo.com/net/SupportPortal/Files/10157/SA234717.pdf

[13] T. Deaconescu, A. Deaconescu, “Pneumatic Muscle Actuated Gripper”, International MultiConference of Engineers and Computer Scientists, Hong Kong 2011, *International Association of Engineers (IAENG), Proceedings vol. II*, pp. 1305-1308, Newswood Limited, Hong Kong.

[14] G. Fantoni, D. Gabelloni and J. Tilli, “How to Design New Grippers by Analogy. Department of Mechanical”, Nuclear and Production Engineering, University of Pisa, Report, 2012.

[15] F. Dudiţă, D.V. Diaconescu, *Textbook of Mechanisms. Kinematics. Dynamics* (in Romanian), Universitatea din Braşov, 1982.